

Kenji Kodama · Kuniyuki Kitagawa

Measurement of two-dimensional distribution profile of lead in a flame by planar laser-induced fluorescence spectroscopy

Received: 14 April 2009 / Accepted: 21 October 2009 / Published online: 16 December 2009
© The Visualization Society of Japan 2009

Abstract Producing refuse-derived fuel (RDF) is one of the most effective measures of refuse treatment. However, RDF often consists of high level of lead. To reduce lead emission during combustion, understanding of lead behaviors in flames is required. In this study, we have applied planar laser-induced fluorescence spectroscopy to detect lead not only in a non-luminous methane–air flame, but also in a luminous RDF flame. In a methane–air flame, the number density of Pb atoms does not depend on the flame temperature, but also on the combustion environments. In RDF flames, because of acceleration of oxidizing process of Pb, Pb fluorescence profile obtained at 25% O₂ became weaker than that at 20% O₂.

Keywords Planar laser-induced fluorescence · Refuse derived fuel · OH radical · Lead

1 Introduction

Refuse-derived fuel (RDF) is a briquette fuel produced from municipal solid wastes. RDF has similar heat energy to brown coal. By producing RDF, low-value municipal solid waste is converted to valuable fuels. Because it produces from municipal solid waste, RDF consists of varied metal elements from daily life of the people; one of these metal elements is lead.

Lead is one of the most familiar metals in our life. However, it is also known as a toxic element. One emission pathway of lead to the environment is combustion. RDF also contains several tens mg kg⁻¹ Pb. Therefore, understanding of lead behaviors in flames is required to reduce toxic emission. Planar laser-induced fluorescence spectroscopy (PLIF) is among the powerful methods for understanding behaviors of chemical species in flames. PLIF enables us to detect not only stable species, but also radical species two dimensionally in flames with narrow monochromatic laser sheet.

In this study, we measured profiles of atomic fluorescence of Pb and molecular fluorescence in a methane–air and RDF flame with a PLIF system operating at a frame repetition rate of 30. From these results, we discuss lead behaviors in flame.

K. Kodama (✉) · K. Kitagawa
EcoTopia Science Institute,
Nagoya University,
Furo-cho, Chikusa-ku,
Nagoya 464-8603, Japan
E-mail: echo@esi.nagoya-u.ac.jp
Tel.: +81-52-7893916
Fax: +81-52-7893910

2 Experimental

2.1 Instrumentation

Figure 1 shows the schematic diagram of the experimental setup assembled for this study. The laser radiation for the Pb or OH excitation is produced using a pulsed Nd:YAG laser and the dye laser (Spectron Laser Systems, SL852G-30 YDA). The tunable dye laser with rhodamine 590 diluted with ethanol is pumped by the second harmonic of the Nd:YAG laser (wavelength of 532 nm, pulse duration of 6 ns, and the pulse repetition rate of 30 pps). The average output power from the dye laser is about 240 mW. The output emission is converted into the ultraviolet radiation for the Pb and OH excitation by the DKDP crystal. The resulting ultraviolet laser beam is transformed into the planar laser sheet beam of about 1-mm thickness and 45 mm in height through a set of cylindrical lenses. The resulting laser sheet beam can intersect any desired cross-sectional area of the flame, including the central longitudinal axis of the burner for excitation of the Pb atoms and OH radicals and provide the 2D cross-sectional fluorescence distribution images of the Pb atoms and OH radicals in the flame.

For the Pb excitation, the dye laser was tuned to 283.3 nm so that the lead atoms were excited from the ground state to the $^7S_{1/2}$ state (resonance line) (Lui et al. 2008). Generally, OH-LIF depends not only on the number density of OH radicals, but also on the temperature. The $Q_1(10)$ rotational line of the $A^2\Sigma^+ \leftarrow X^2\Pi(1,0)$ transition (wavelength of 284.3 nm; Dieke and Crosswhite 1962) is selected as the OH excitation line with negligibly small temperature dependency.

The 2D distribution of the Pb or OH fluorescence intensity is monitored with the ICCD camera (PCO Computer Optics GmbH, DiCAM-PRO, 320×240 pixels). The interference filters (Andover Corporation, 305FG01-50 and 005FG09-05) are attached to the lens (UV-NIKKOR, $f = 105$ mm) of the camera for blocking-off the laser emissions. The full width at half maximum (FWHM) of the filters is 360 ± 50 nm, which covers the Pb-PLIF (364.0, 368.4 and 405.8 nm) and OH-PLIF band (ca. 305–330 nm) selected in this measurement. The digital delay and pulse generator system (Stanford Research Systems, Model DG535) is used to effectively attenuate the interference from the undesirable scattering radiation by controlling the pulsed Nd:YAG laser and the ICCD camera. The accumulation of 200 individual PLIF images is conducted to reduce the influence of flame fluctuation on the image.

2.1.1 Methane–air flame

A methane–air premixed flame was formed on a cylindrical fused-silica burner of 8 mm i.d. The resulting flame was ca. 40 mm in height. The burner is connected to a spray chamber that prevents larger aerosol droplets from reaching the flame (Fig. 2). The nebulizer supplies sample aerosols into the spray chamber. The flow rate of each component in the premixed gas at the burner outlet is listed in Table 1.

The 2D temperature distributions were measured with a R-type thermocouple of 4 mm in diameter. The measurements were made at three points from -4 to 4 mm at 4-mm intervals in the radial direction (r), and nine points from 0 to 32 mm at 4-mm intervals in the longitudinal direction (z), respectively. An x – z stage is used to move the thermocouple relative to the fixed burner position.

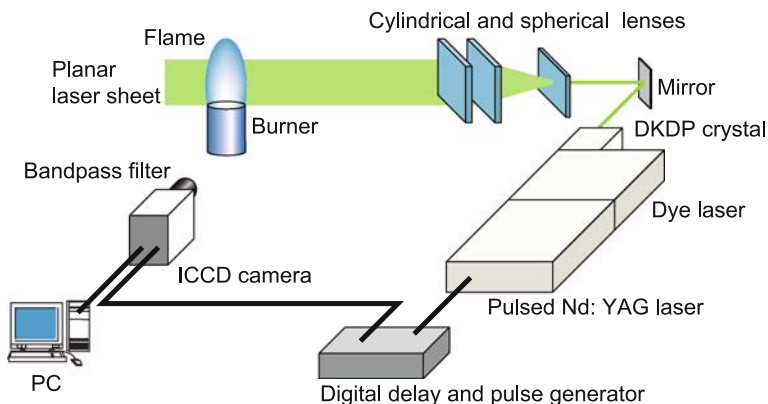


Fig. 1 Experimental setup of PLIF system

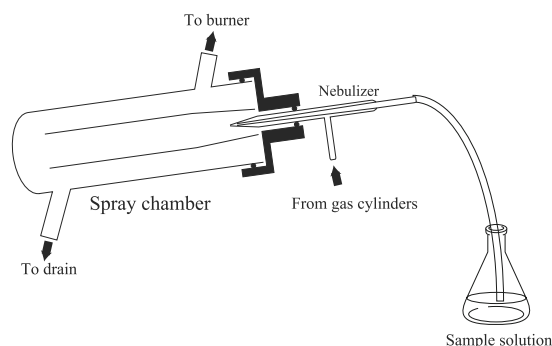


Fig. 2 Schematic diagram of spray chamber

Table 1 Equivalence ratio and gas flow rate for methane–air premixed flame

ϕ	CH ₄ (cm ³ min ⁻¹)	Air (cm ³ min ⁻¹)
0.73	150	1,950
1.0	200	1,900
1.3	250	1,850

2.1.2 RDF flame

An RDF flame was formed using the cylindrical fused-silica burner that incorporates alumina grains (5 mm in diameter) at the upstream location so as to improve air flow distribution at the burner exit. The burner details are shown in Fig. 3. The mixture gas of O₂ and N₂ was supplied from the bottom of the burner. The RDF sample was filled in the upper part of burner. The sample weight of the RDF used for combustion was 3.00 ± 0.05 g.

2.2 Sample

For the test measurement of the methane–air premixed flame, a standard solution of 10 g Pb dm⁻³ sample solution was prepared by dissolving lead (II) nitrate of analytical grade in deionized water. The RDF tested in this work was provided from clean park WAKASUGI, Fukuoka, Japan. The typical compositions of RDF are listed in Table 3. RDF sample was crushed to 1–5-mm diameter size pellets. To facilitate detection of Pb profile, 100 mg kg⁻¹ Pb as lead (III) nitrate was added to the RDF samples.

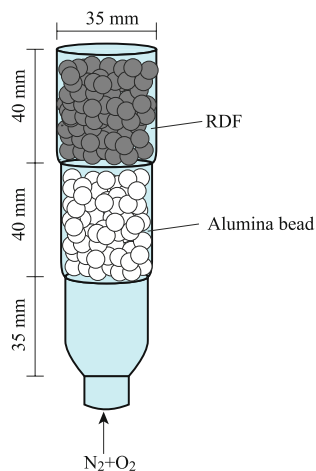


Fig. 3 Schematic diagram of burner for RDF flame

Table 2 Gas flow rate for RDF flame

	O ₂ (dm ³ min ⁻¹)	N ₂ (dm ³ min ⁻¹)
20% O ₂	0.8	3.2
25% O ₂	1.0	3.0

Table 3 Typical compositions of RDF

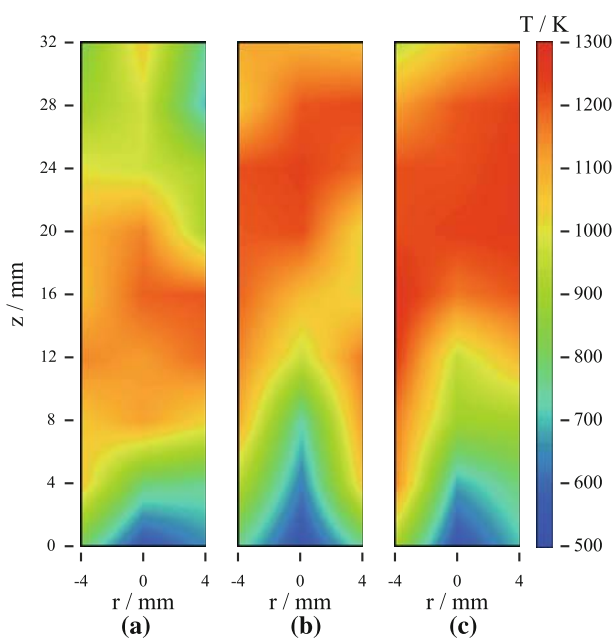
Water (%)	3.7–5.8
Volatile (%)	79.3–82.9
Ash (%)	13.4–14.9
Chloride (%)	0.2–0.3
Nitrogen (%)	0.9–1.5
Mercury (mg kg ⁻¹)	0.09–0.87
Cadmium (mg kg ⁻¹)	1.1–1.7
Chromium (mg kg ⁻¹)	21–39
Lead (mg kg ⁻¹)	56–150

3 Results and discussion

3.1 Methane–air flame

Figure 4 shows the 2D profiles of flame temperature measured with the R-type thermocouple at equivalence ratios of $\phi = 0.73$, 1.0 and 1.3. Figure 5 shows a comparison of two-dimensional distributions of Pb fluorescence intensity in methane–air flames at the different fuel equivalent ratios. If atomization is ruled only by thermal dissociation processes, its degree is simply dependent on the flame temperature. However, from Figs. 4 and 5, it is found that the fluorescence profiles of Pb were not quantitatively correlated to the flame temperature profiles.

Figure 6 shows a comparison of two-dimensional distributions of OH fluorescence intensity in methane–air flames at the different fuel equivalent ratios. The comparison between Figs. 5 and 6 indicates the fluorescence intensity of Pb, which is correlated inversely with that of OH radicals. The fluorescence profiles of OH radicals reflect an oxidizing environment in the flame. Therefore, this correlation suggests that the number density of Pb atoms does not depend on flame temperature, but also on such environments as redox, etc. in the flame.

**Fig. 4** 2D distribution of flame temperature of different fuel equivalence. **a** $\phi = 0.73$, **b** $\phi = 1.0$, **c** $\phi = 1.3$

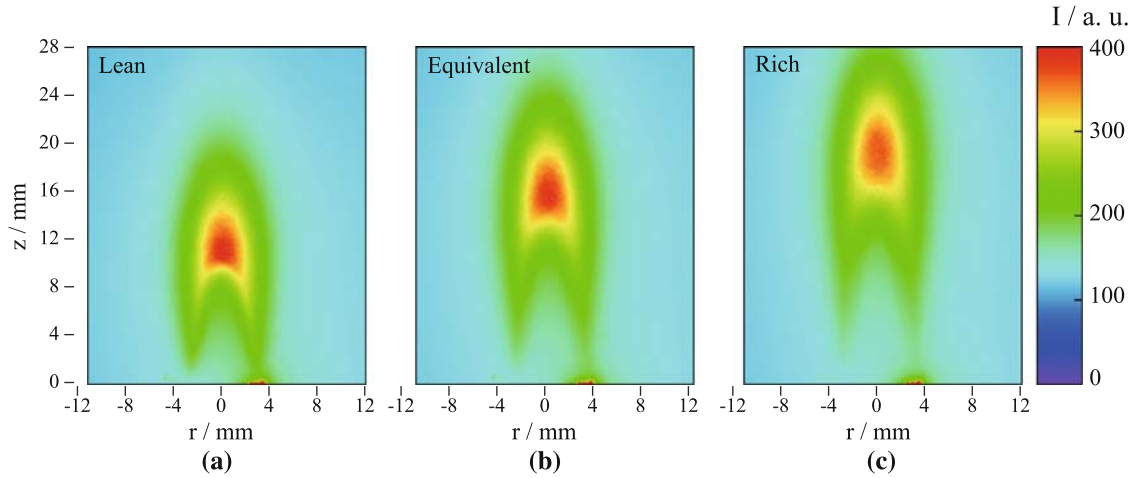


Fig. 5 2D distribution of Pb fluorescence intensity of different fuel equivalence. **a** $\phi = 0.73$, **b** $\phi = 1.0$, **c** $\phi = 1.3$

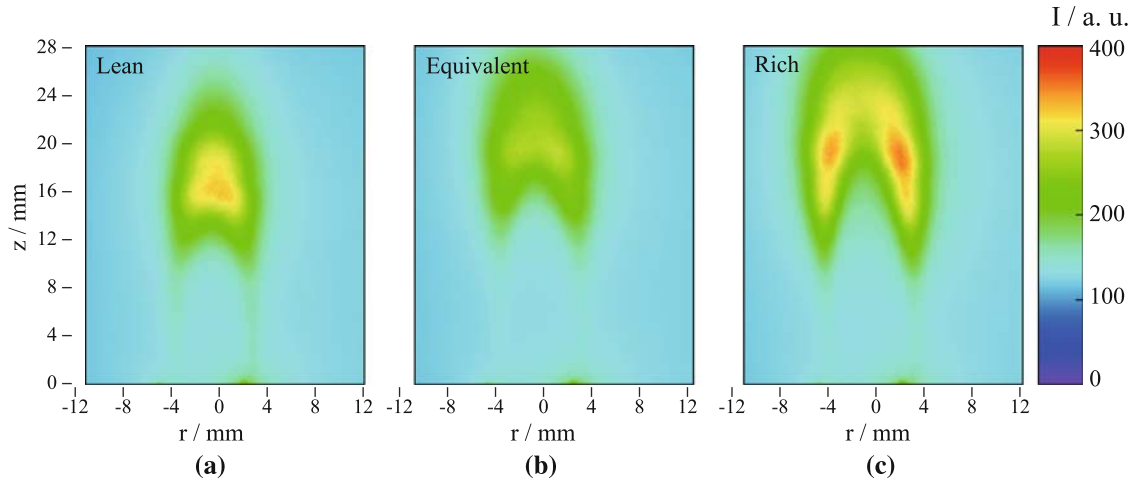


Fig. 6 2D distribution of OH fluorescence intensity of different fuel equivalence. **a** $\phi = 0.73$, **b** $\phi = 1.0$, **c** $\phi = 1.3$

3.2 RDF flame

Because the methane–air premixed flame was a non-luminous flame, it was easy to take LIF profiles. On the other hand, the RDF flame was a luminous flame containing high density particles of soot precursors. The laser sheet beam, therefore, is strongly scattered by the particles. Although direct detection of laser beam is limited with the bandpass filter and the delay generator, it is difficult to totally remove the signals of scattered laser radiation. To overcome this problem, background profile of slightly different wavelength from Pb resonance line was taken. Because the LIF technique is very sensitive to the tuned excitation wavelength, the fluorescence signals are not detected by slight difference of wavelength. Although scattering by particles is almost insensitive about wavelength. It is considered that gross fluorescence profiles of Pb include a net Pb fluorescence and scattering. On the other hand, the background profiles include only scattering in the luminous flame. The net fluorescence profiles of Pb, therefore, can be obtained by subtracting the background profiles from the gross Pb ones. Figures 7, 8 and 9 show the profiles of gross fluorescence profiles of Pb, the background scattering profiles and the net fluorescence profiles of Pb, respectively. The profiles obtained by supplying 20% O₂ mixture gas (N₂: 3.2, O₂: 0.8 dm³ min⁻¹) and 25% O₂ mixture gas (N₂: 3.0, O₂: 1.0 dm³ min⁻¹) are shown in a and b, respectively. Figure 8 shows that the scattering profile of 25% O₂ was more diffusible and intensive than that 20% O₂. This result suggests that combustion reaction and soot production were accelerated in the oxidizing atmosphere of the flame. Despite the combustion reaction was accelerated, the net Pb fluorescence profile obtained with 25% O₂ was

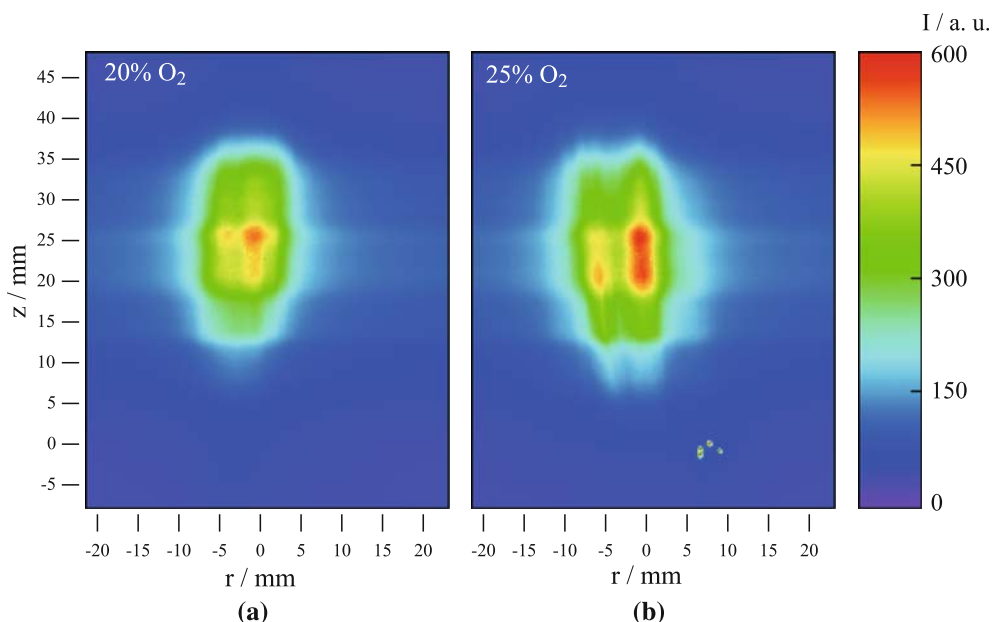


Fig. 7 2D distribution of gross Pb fluorescence intensity of different fuel equivalence. **a** N₂: 3.2, O₂: 0.8 dm³ min⁻¹, **b** N₂: 3.0, O₂: 1.0 dm³ min⁻¹

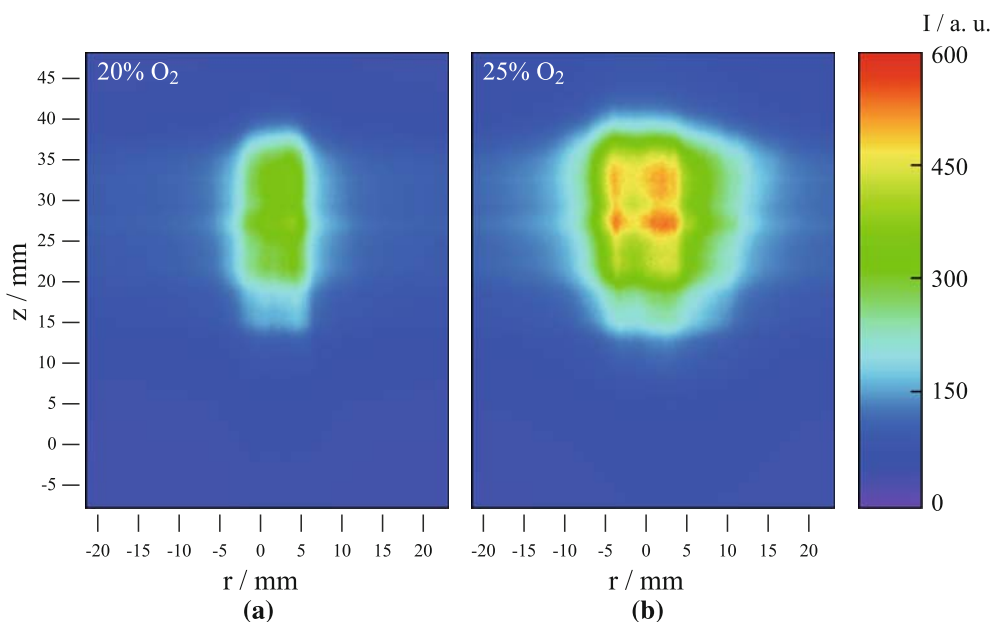


Fig. 8 2D distribution of background scattering intensity of different fuel equivalence. **a** N₂: 3.2, O₂: 0.8 dm³ min⁻¹ **b** N₂: 3.0, O₂: 1.0 dm³ min⁻¹

weaker than that with 20% O₂ (Fig. 9). The result of methane–air flame indicate the number density of Pb atoms is lower under the oxidizing environments. The reasonable explanation for this is that the environment of 25% O₂ flame was more oxidizing in the atomization reaction of $\text{PbO} \rightleftharpoons \text{Pb} + \text{O}$ than that of 20% at O₂. Consequently, the net Pb fluorescence profile at 25% O₂ became weaker.

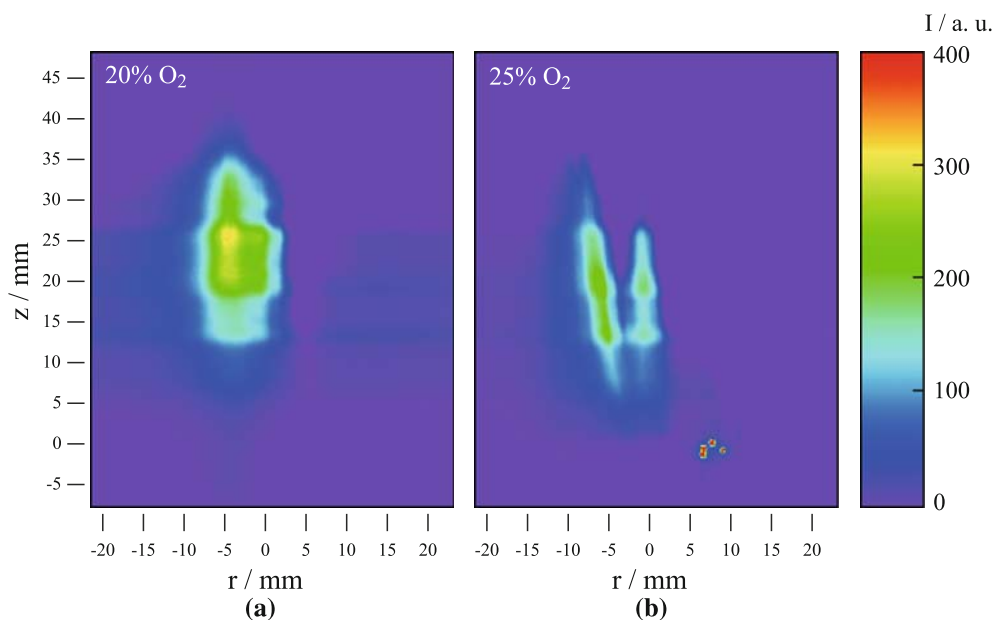


Fig. 9 2D distribution of net Pb fluorescence intensity of different fuel equivalence. **a** N_2 : 3.2, O_2 : 0.8 $\text{dm}^3 \text{min}^{-1}$, **b** N_2 : 3.0, O_2 : 1.0 $\text{dm}^3 \text{min}^{-1}$

4 Conclusion

The results presented in this study demonstrate that two-dimensional distribution of Pb atom was successfully detected not only in the non-luminous flame of methane–air, but also the luminous flame of RDF. Net Pb fluorescence profiles indicate that the environment of 25% O_2 RDF flame was more oxidizing in the atomization reaction of $\text{PbO} \rightleftharpoons \text{Pb} + \text{O}$ than that of 20% at O_2 . This technique is effective to understand behaviors of toxic elements in various flames.

References

- Dieke GH, Crosswhite HM (1962) The ultraviolet bands of oh fundamental data. *J Quant Spectrosc Radiat Transf* 2(2):97–199. doi:[10.1016/0022-4073\(62\)90061-4](https://doi.org/10.1016/0022-4073(62)90061-4)
- Lui SL, Godwal Y, Taschuk MT, Tsui YY, Fedosejevs R (2008) Detection of lead in water using laser-induced breakdown spectroscopy and laser-induced fluorescence. *Anal Chem* 80(6):1995–2000